



**COB-2021-XXXX (XXXX is the identification number of the final paper)**  
**CHALLENGES IN THE MANUFACTURING OF A CRYOGENIC  
COOLING MANIFOLD FOR AN X-RAY MONOCHROMATOR AT SIRIUS  
LIGHT SOURCE**

**Marlon Saveri Silva**

**Ricardo Luiz Parise**

**Renan Ramalho Geraldes**

Brazilian Synchrotron Light Laboratory, LNLS, CNPEM. 13083-100, Campinas, Brazil

[marlon.saveri@lnls.br](mailto:marlon.saveri@lnls.br), [ricardo.parise@cnpem.br](mailto:ricardo.parise@cnpem.br), [renan.geraldes@lnls.br](mailto:renan.geraldes@lnls.br)

**Abstract.** *The current work discloses and details the solutions for the challenges in manufacturing a liquid nitrogen distribution circuit carefully designed to minimize the flow-induced vibrations in cryocooling the High-Dynamic Double-Crystal Monochromator (HD-DCM), an optical instrument responsible for selecting specific narrow energy bands from broad-band photon beams at Sirius – the 4<sup>th</sup>-generation synchrotron light source in the Brazilian Synchrotron Light Laboratory (LNLS) at the Brazilian Center for Research in Energy and Materials (CNPEM). The design relies on modal and computational fluid dynamics (CFD) simulations and on the selection of appropriate materials and processes, contributing to the development of an innovative national piece of technology. The elaborated geometry of the main manifold was achieved by means of additive manufacturing in AISI 316L, which needed to be validated for ultra-high vacuum (UHV) compatibility. The oxygen-free copper heat sinks that make actual contact with the main optical elements, namely, diffracting silicon crystals, in turn, were manufactured via vacuum brazing processes at different temperatures. Finally, the union of the small stainless-steel distribution pipes between the manifold and the copper heat-sinks was made by laser welding. The final product shows how the association of different techniques has led to a successful result, since the circuit is currently in operation in the HD-DCM at the Extreme Condition X-Ray Method of Analysis Beamline (EMA), with validated UHV compatibility, and cooling and dynamic stability performances. Now, new distribution circuits based on the developed technology are currently in design for future DCM models. This study also compares the manufacturing process of this successful solution with previous versions.*

**Keywords:** *additive manufacturing, brazing process, welding process, cryogenic cooling, synchrotron radiation*

## 1 Introduction

Sirius light source, located in the Brazilian Synchrotron Light Laboratory (LNLS), is the most complex scientific infrastructure in Brazil, delivering electromagnetic radiation from Infrared to hard X-rays to be applied to diverse experimental techniques to study materials in micro and nano scale (Westfahl, 2018).

Monochromators are optical instruments responsible for the selection of specific energy bands, which makes them an item of critical importance in most of the synchrotron research stations, the so-called beamlines. MANACA (Macromolecular Micro and Nano Crystallography) and EMA (Extreme Condition Methods of Analysis) are two of the first Sirius beamlines, enclosing a particular class of monochromators, the so-called High-Dynamic Double-Crystal Monochromator (HD-DCM) (Geraldes, 2018), whose third and fourth unities are in development for the future beamlines QUATI (Quick X-Ray Absorption Spectroscopy for Time and Space Resolved Experiments) and SAPUCAIA (Small Angle X-ray Scattering).

The HD-DCM uses the rotation of a pair of silicon crystals to provide the energy selection according to the Bragg's law of diffraction. The second crystal receives the monochromatic beam that is primarily diffracted by the first, such that, following its rotation and being appropriately translated with respect to it, a constant offset can be kept in the propagation of the downstream monochromatic X-ray beam with respect to the upstream broad-band beam. To keep the parallelism between the crystals in the order of tens of nanoradians, so that the position stability of the X-ray beam in the experimentation stations is ensured – both for fixed-energy operation and during energy scans –, the HD-DCM design process adopted a successful predictive modelling approach based on a high-bandwidth closed-loop control. A combination of high-stiffness parts and mounts with a few low-stiffness flexible interfaces allows not only for the desired dynamic behavior, but also for handling large temperature gradients and differences in thermal expansion. By design, two pairs of crystals with different lattice parameters are included side-by-side, as seen in Figure 1a. Thus, by translating the entire instrument, the user can choose which pair receives the incoming X-ray beam (active set) and, consequently, a monochromatic beam from a different energy range and with a different energy resolution.

First and second crystals of both sets are kept at 77 and 155 K respectively, aiming to preserve optical properties by reducing mechanical deformations on the beam footprint. Indeed, up to 135 W can be absorbed from the incoming beam by the active first crystal, with power densities reaching up to 50 W/mm<sup>2</sup>. Hence, they are indirectly cooled by being clamped between copper heat sinks consisting of cooling blocks with small internal channels flowing liquid nitrogen. As shown in Figure 1b, the flow is distributed to the cooling blocks by small-diameter stainless steel pipes derived from an additive-manufacturing stainless-steel cooling manifold (CMF), which is placed between the metrology frame that holds the first crystals of both sets and the auxiliary frame 1 (AF1) that is finally connected to the rotary stage (not shown). The second crystals, in turn, are subject to much lower power loads and require a less demanding cryocooling solution, which is implemented by means of copper braids connected to the main cooling circuit.

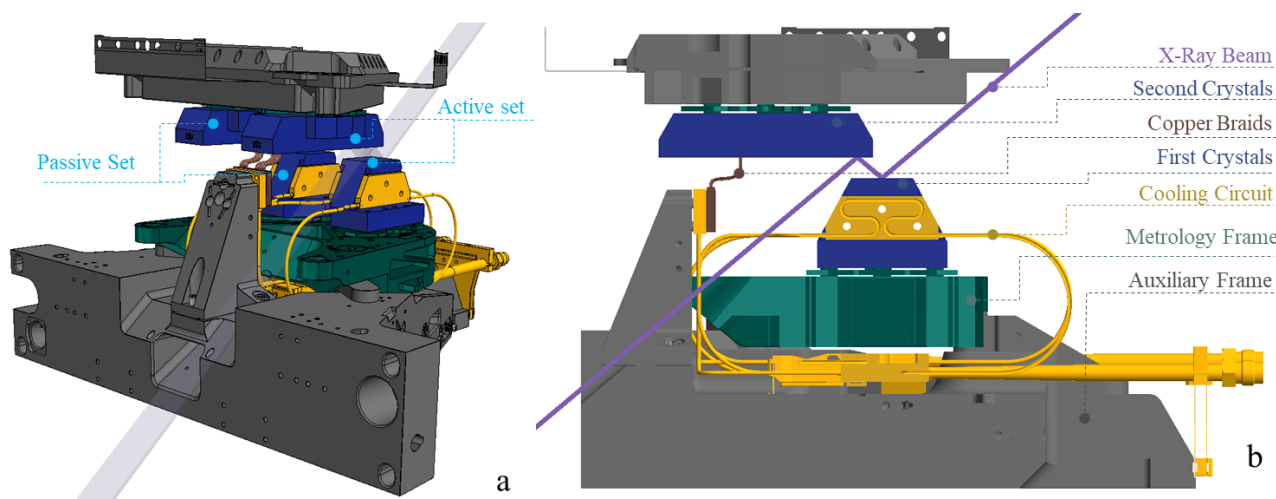


Figure 1. Perspective (a) and side (b) views of the neighborhood of the cooling circuit in the new HD-DCMs, which are under design phase for QUATI and SAPUCAIA beamlines. The active and passive sets are shown and the main components of interest are highlighted: first and second crystals, cooling circuit, metrology and auxiliary frames for the first crystals, and copper braids for the second crystals. A representation of the X-ray beam being diffracted by the active pair of crystals at a given angle is shown for reference.

Solutions for the union between dissimilar materials in ultra-high vacuum (UHV) environment, which have long been part of the scope of the LNLS Materials Group (Bagnato, 2011), together with additive manufacturing techniques for stainless-steel parts that have been developed over the last decades, were fundamental to the implementation of the complex internal geometries in the HD-DCM solution, as detailed in the following sections.

## 2 MECHANICAL DESIGN

The choice for an indirect cooling solution instead of flowing the liquid nitrogen inside the crystals was made due to the risks associated to leakage and vacuum tightness, the path length limitation, and the complexity of brazing silicon crystals to a metallic fitting (Auricchio, 2019).

Figure 2 shows the CAD drawing and the pictures of the circuits installed at MANACA and EMA, which were the first to be produced and are currently in operation. The cooling blocks are made of oxygen-free copper due to its high conductivity and UHV brazing compatibility. The cooling circuit is fixed to the frame AF1 through flexible Ti6Al4V foils, which are designed to allow for the thermal contraction of the CMF to a thermal center, while keeping limited heat leakage from the AF1 and also all eigenfrequencies above 800 Hz when assembled to the crystals. All other parts are made of stainless-steels AISI: 316L for the CMF and 304 for all the pipes, inserts and clamping parts.

The main difference between MANACA and EMA to QUATI and SAPUCAIA designs is the number of cooling paths between the CMF and each cooling blocks associated to the crystals, addressed as CB1s. For the first two beamlines, each CB1 has two inlets and two outlets, such that two cooling paths run liquid nitrogen in opposite directions to better balance the disturbance forces induced by the flow and to optimize heat extraction capacity. However, the X-ray beam that will hit QUATI's crystals is larger and, as consequence larger crystals were necessary occupying more space. Fortunately, QUATI X-ray beam delivers lower heat load (54 W) when compared to MANACA and EMA (135 W). Thus, the CB1s could be reduced, presenting only one inlet. Even though the larger crystal would not be necessary to SAPUCAIA, the beam that hits it also presents a smaller heat load (<80 W) and a standard solution was adopted to both new DCMs. In all designs, an additional cooling block, referred to as the cooling manifold extension (CMX), has one inlet and one outlet, and is used for the connection of the copper braids (Lena, 2021) as the cryogenic heat sink for the second crystals.

The internal and external diameters of the distribution pipes connecting the CMF to the CB1 and to the CMX are 2 and 2.5 mm, respectively. The choice for thin and sufficiently long pipes aimed at minimizing the mechanical coupling

between the CMF and the first crystals, in addition to fitting in the available space, considering the X-ray beam path and other components of the instrument. Another small difference between designs lies in the main inlet and outlet tubes of the CMF. For MANACA and EMA they are cylindrical tubes with internal and external diameters of 7 and 9 mm, respectively, whereas for QUATI and SAPUCAIA they are conical tubes with the internal diameter varying between 7 and 4.35 mm for flow smoothness over different connection sizes. In all cases, these pipes are connected via 3/8" VCR fittings to the external liquid nitrogen supply via corrugated flexible pipes. Indeed, there is no separation in whole liquid nitrogen path in the cooling circuit, which is a conceptual choice to minimize: vibration sources in interfaces, reduce masses and volumes, and mitigate leakage possibilities. The price to be paid was the development concerning the design, the UHV compatible process and the junction of dissimilar materials.

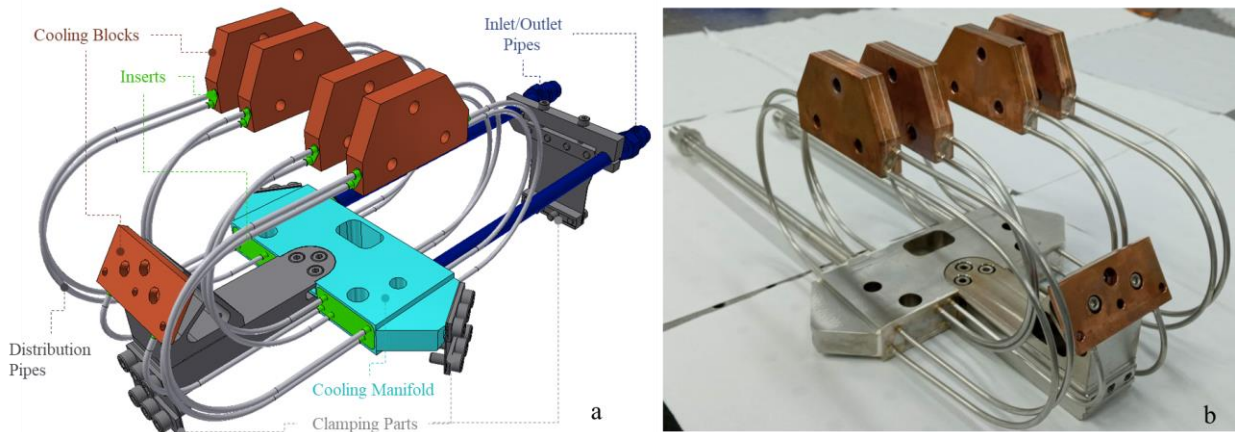


Figure 2. Drawing (a) and picture (b) of the cooling circuits installed at MANACA and EMA beamlines, highlighting the cooling manifold, cooling blocks with two paths, inlet, outlet and distribution pipes, inserts, and clamping parts.

In particular, considering different manufacturing process and development challenges, several designs have been elaborated for the CMF. **Erro! Fonte de referência não encontrada.** Figure 3 depicts four different designs comprising the solutions for the MANACA/EMA and QUATI/SAPUCAIA beamlines. In all of them the internal channels of the CMF were arranged in a way to equally distribute the liquid nitrogen flow to the parts. Yet, with conventional machining, only simplified designs are possible for the channels, whereas with additive manufacturing smooth arterial shapes are possible, reducing pressure drop, recirculation and abrupt changes in flow speed. Within the additive manufacturing perspective, considering leak tightness risks over thin walls and the surface finishing aspects related to large rough areas, only simple holes and milled sections have so far been used for weight reduction, rather than more sophisticated mass relief options that could be designed in as the non-adopted proposal shown in Figure 3d.

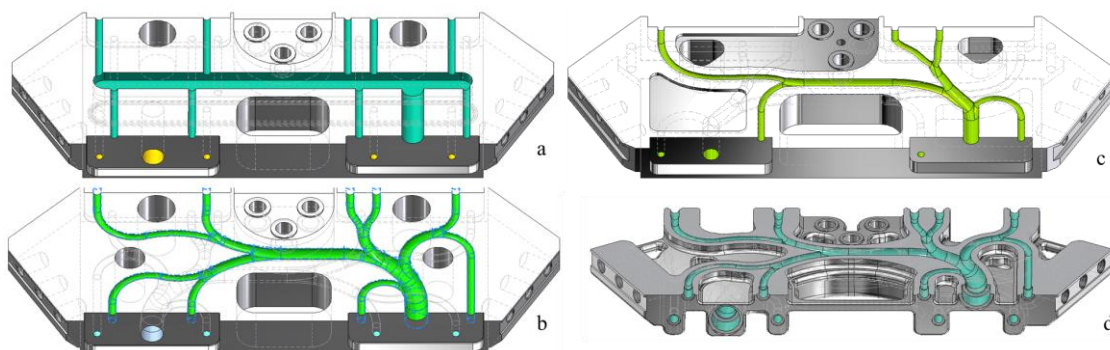


Figure 3 - Section view of cooling manifolds (CMFs): simplified (a), MANACA/EMA (b), QUATI/SAPUCAIA (c) and potential lighter (d) versions.

### 3 Thermo-mechanical Simulations

To comply with the requirements in the dynamic architecture of the HD-DCM, the target was to have the eigenfrequencies of the cooling circuit above 800 Hz (preferably even above 1kHz), which required extensive work on modal analyses. Since the distribution pipes have low stiffness, i.e., less than 1 kN/m between their fixed ends for x-y-z translations, and the CB1s are directly clamped to the crystals, the parts were simulated in two groups.

In the first group, the clamping between the CMF and the AF1 frame was evaluated, and the clamping foils were chosen according to the compromise between the required high eigenfrequencies, low thermal conductance, and acceptable stresses due to thermal contraction. This last condition motivated the use of Ti6Al4V foils. Figure 4 shows the first eigenfrequency, the temperatures and the deformations simulated in Ansys for QUATI/SAPUCAIA versions. The contact stiffness among parts and the elastic clamping to the AF1 frame were assumed as 500 MN/m for each direction, whereas the thermal conductance in the interfaces were estimated as 2 kW/m<sup>2</sup>K. After that, these parts were simulated along with the other parts within the module of the first crystals, resulting in the first eigenfrequency also above 800 Hz.

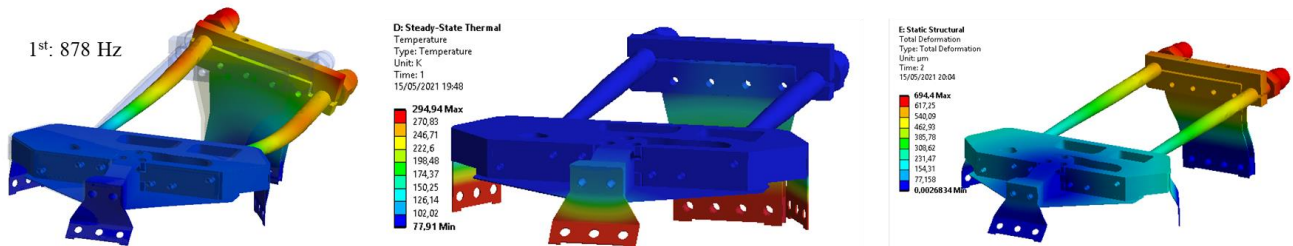


Figure 4 - First eigenfrequency (left), temperature distribution (center) and deformation (right) due to thermal contraction for QUATI/SAPUCAIA cooling circuit version.

Computational fluid dynamics (CFD) was firstly performed to double-check estimates of heat transfer coefficient previously got by analytical methods and to evaluate pressure drop to analyze requirements of the source of liquid nitrogen. Furthermore, pressure drop analysis, associated to the temperature distribution delivers information about boiling and, the velocity distribution, about the turbulences. Besides the eigenfrequencies of the structure, flow induced disturbances can also affect the dynamic behavior of the system through acoustic resonance, turbulence, vortexes, pressure pulsation or phase changes (Moreno, 2010; Wetering, 2019).

In the simulation of Figure 5, made in Ansys CFX for QUATI parameters, the fluid enters at 77 K at 1.7 L/min and leaves the set at 2 bar. A total of 54 W is removed from the active crystal, whereas only 2 W is extracted from passive crystals. Moreover, 16 W are introduced in the CMX due to the heat flow from the second crystals set and from the AF1 frame. The result shows that there is no sudden velocity change, with a homogenous flow distribution along the four CB1s, which was obtained after a few interactions between CFD and design. A pressure drop of only 0.14 bar was obtained, which should avoid boiling since the temperature never goes above vaporization temperature for the considered pressure (Chelton, 2010). The average heat transfer coefficient was simulated as 6kW/m<sup>2</sup>K on the CB1s and 4kW/m<sup>2</sup>K on the CMX, close to the expected by Gnielinski correlation (Incropera, 2012).

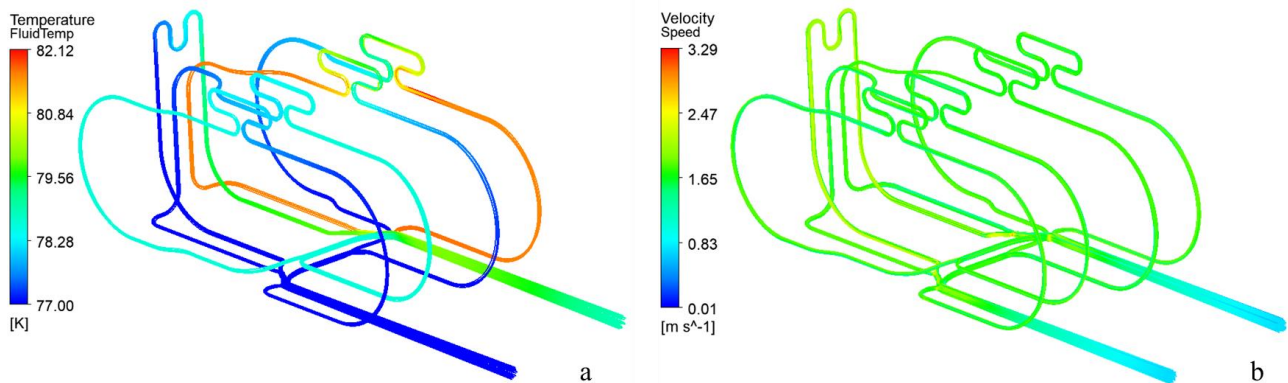


Figure 5 – CFD analysis of liquid nitrogen flow for the QUATI case: (a) fluid temperature; (b) fluid velocity homogeneously distributed among the channels with a smooth acceleration along inlet and outlet pipes.

Flow induced vibrations was investigated in dedicated works (Caliari, 2016; Wetering, 2019) to be used as input in the HD-DCMs dynamic modellings. The complexity of the geometries, space and manufacturing limitations, and the need of a high heat transfer coefficient demotivated the pursuit of a solution in laminar regime and a low turbulent regime was adopted. The stand-still position stability between the crystals (also referred to as in-position stability) was evaluated to the MANACÁ DCM (Gerales, 2018) and the additive manufactured CMF (Figure 3b) allowed for a positioning error reduction in a factor of 2 when compared to the machined version (Figure 3a).

## 4 Manufacturing processes

As depicted in Figure 6, the current manufacturing process is divided in eight sub-steps: A) brazing and machining of the cooling blocks; B) additive manufacturing and machining of the CMF manifold; C) cutting, bending and laser welding of the tubes; D) manufacturing of parts for clamping, alignment and leak testing; E) nickel-plating on stainless-steel brazed parts; F) brazing of full system final; G) final assembling; and H) testing with pressure and cooling. Along with that, leak tests with helium gas were conducted after each applicable step. This subdivided process facilitated the improvement of each sub-step part or process involved by allowing a focused in-house development or a careful outsourcing process. All these steps are detailed in the following subsections.

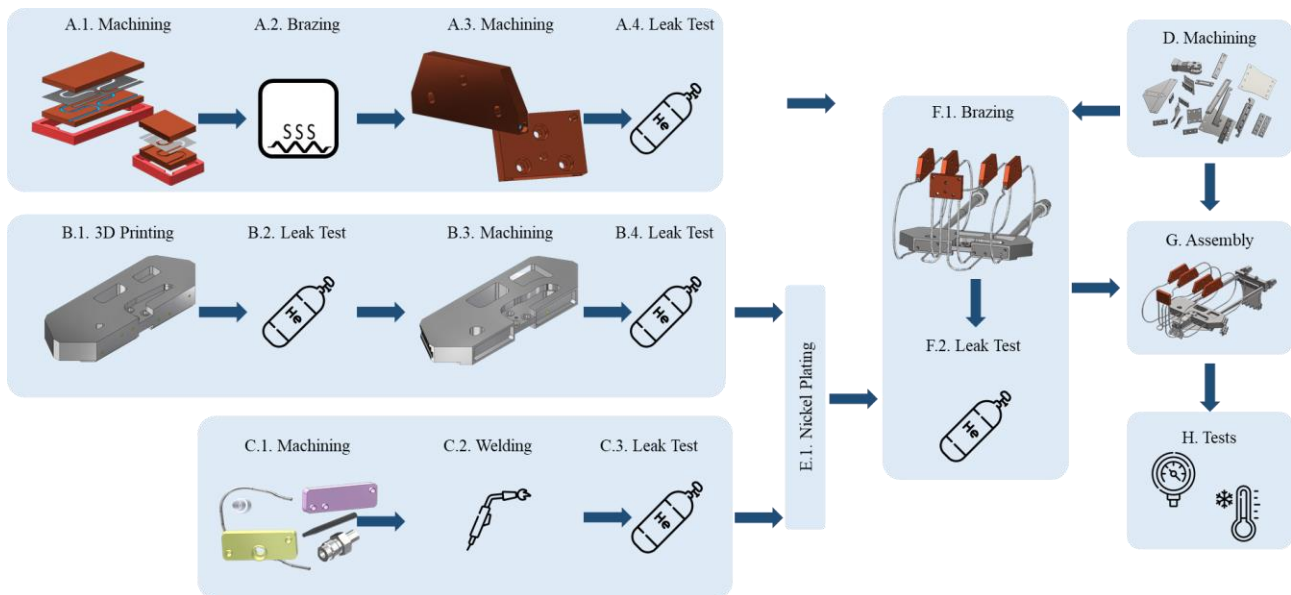


Figure 6 - Manufacturing steps: (A) manufacturing of the cooling blocks, (B) manufacturing of the manifold (CMF), (C) manufacturing of pipes and inserts, (D) machining of complementary parts, (E) nickel plating, (F) brazing, (G) final assembling, and (H) testing.

### 4.1 Manifold: Additive Manufacturing and Machining

The first attempt to construct the CMF was by vacuum brazing three stainless-steel machined plates with half round channels in a way to build the internal channels. This option requires tight flatness tolerances on large nonmagnetic surfaces, which was not possible due to the warping of these flat surfaces during the machining what prevented the final brazed manifold to be vacuum-tight.

The additive manufactured parts, shown in Figure 7, were developed and produced by the company *Fábrica de Protótipos* associated to the University of Campinas and achieved a suitable result by using the Direct Metal Laser Sintering (DMLS) technique on AISI 316L stainless-steel. The main challenge was to build a dense and non-porous piece that could be used in a vacuum environment. After an iterative process, the parameters were optimized to an UHV compatible material.

The development started with the additive manufacturing of small samples (10 x 10 x 25 mm) with a single round channel with an internal diameter of 2 mm. These first samples were porous and presented leak rates of 1e-3 mbar.l/s. Hardness tests showed a similar mechanical behavior for these additive manufactured samples in comparison with 316L blanks. The surface roughness was higher than the recommended UHV applications and a tumble finishing was conducted to reduce it, yet it was not effective. After that, the company *Fábrica de Protótipos* carried out an inner process to reduce the porosity and enhance the density of the parts. The parameters explored were the power of the laser, the speed, and the printed layer thickness. Following these improvements, small samples were leak tested and achieved 1e-11 mbar.l/s, being approved for applications in UHV.

The next step was to manufacture the actual manifold with two layers of complex internal channels (see Figure 3b) and the final external dimensions. The first approach was to build a near-to-finish part, with 1 mm of extra material to be removed by machining in order to ensure the final dimensions with low roughness. The manufacturing orientation chosen was with the plane of the channels perpendicular to the machine table. This resulted in a distorted part with poor dimensional precision. Due to that, both the manufacturing orientation and the extra material quantity were changed. The following test was manufactured with the plane of the channels parallel to the machine table and 3 mm of extra material was added to the part which improved both the external and the channels dimensions. However, after removing it from the table, it was noticed that the part was warped. The final solution to the warping issue was a heat treatment conducted

prior to the part removal from the table, which consisted in heating the full set up to 400°C in a vacuum furnace, followed by a slow cooldown.

A side effect of the heat treatment was that remaining powder inside the channels clustered and partially blocked the flow. To avoid this obstruction to be permanent, an additional step of cleaning was included before the treatment. It consisted of blowing pressured air inside the channels and a following ultrasonic bath with isopropanol.

Another concern was the internal roughness of the channels, which could increase the turbulence in the cooling system, especially on the upper side of the channel, that does not have support structures and tends to be rougher. To reduce this issue, a design for additive manufacturing (DfAM) technique was studied and evaluated (Zluhan, 2019). It was proposed a drop shaped channel design instead of the regular round shaped channel design. However, a similar roughness was observed in both round and drop shaped channels. Hence, the round shaped channel design was chosen for being more adequate for thermal fatigue.

After the process development, two batches of final parts following the best practices were made. Leak tests were performed before and after the final machining to validate its usage in the next steps.

The additive manufacturing of the CMF is responsible for approximately 45% of the total cost of the manufacturing of the cooling system but represents a tiny fraction of the costs of the machining of the entire equipment, justifying the additional investment by the positive impact of the smooth paths in the positioning stability performance of the HD-DCM.

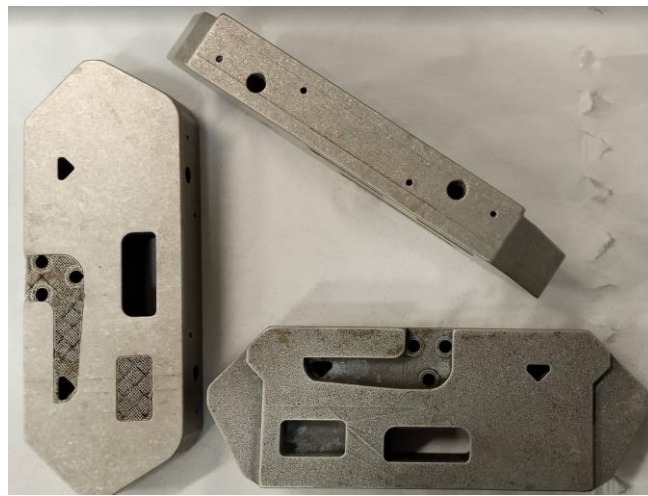


Figure 7 – Additive manufactured manifolds of QUATI and SAPUCAIA before being machined.

#### 4.2. Cooling Blocks Brazing and Machining

To manufacture a bulky block with internal round channels, half-round channels were machined in flat copper plates and then vacuum brazed. A first approach to ensure the alignment of the half-round channels was with male/female coupling. Although it resulted in well aligned channels, some leak problems were detected due to the lack of contact between the flat surfaces, which was caused by interference between the sharp edges of male parts and the tool radius of female parts. A successful design was obtained by using mirrored copper parts and an alignment guide, also made of copper, with strict machining clearances, as shown in Figure 8.

The vacuum brazing was performed using 0.1mm-thick sheets of Pd-Cu-Ag brazing alloy (BVAg-31), which has a melting temperature in the range of 810 and 885°C. This brazing alloy was chosen due to its good copper wettability, vacuum compatibility and high melting temperature, which allowed for a second brazing step for the complete cooling system using a lower melting temperature alloy. It took place in a vacuum furnace with inner atmosphere of 1e-5 mbar. Heating up was performed with a heating rate of 3°C/minute and the temperature was measured and controlled with two thermocouples. Prior to the brazing process, the copper and the brazing alloy parts were cleaned in a standard UHV cleaning procedure, with alkaline detergent and ultrasonic bath, and the copper parts were etched with a 10% sulfuric acid aqueous solution. The whole brazing process was an in-house development. After the brazing process, the cooling blocks were machined to the final dimensions and leak test was performed to approve their usage in the following steps.

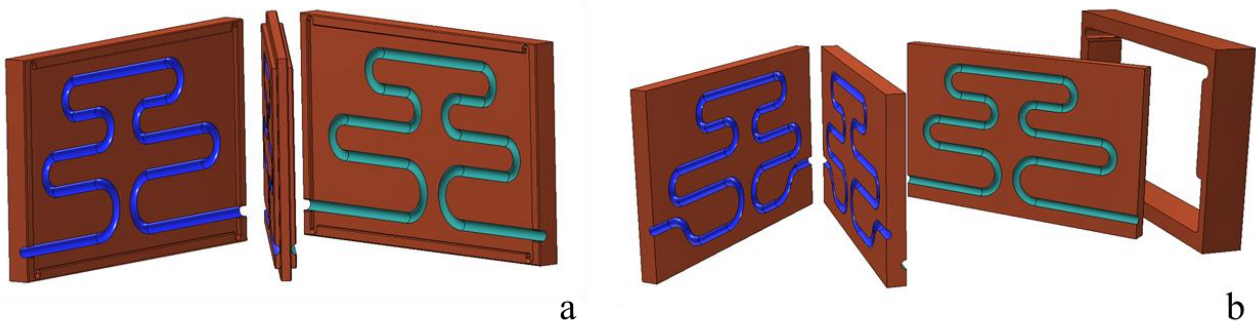


Figure 8 - Preliminary (a) and final (b) designs of the parts that compose the cooper cooling blocks (CB1s) of MANACA and EMA cryogenic circuits.

### 4.3. Tubes Laser Welding

Laser welding was used to bond the stainless-steel tubes to the so-called inserts, also made of stainless-steel. This welding technique was chosen due to the small tube diameter (2.5 mm) and to the thin tube walls (0.25 mm). The first steps of the manufacturing process were the cutting and bending of the tubes and the machining of the inserts. These insert parts were designed to increase the brazing area in the following step of the manufacturing process to ensure vacuum tightness. After that, the bended tubes and the inserts were fixed with alignment devices and laser welded in a manual process. The cutting and bending were done by the company *Matool Usinagem de Precisão* and the laser welding by *FCA Brasil*. Leak tests were performed to approve its usage in the following steps.

Previous versions had been manufactured without the stainless-steel inserts and the tubes were brazed directly to the cooling blocks, as in described in Figure 9. Although it avoided the need of the laser welding, several issues related to the correct alignment of the tubes and vacuum tightness were faced. Indeed, without the inserts the last brazing operation would involve 38 brazing points for MANACA/EMA and 22 points for QUATI/SAPUCAIA, whereas only 14 points remain when the inserts are included and previously welded. The welded regions are zoomed in Figure 10.

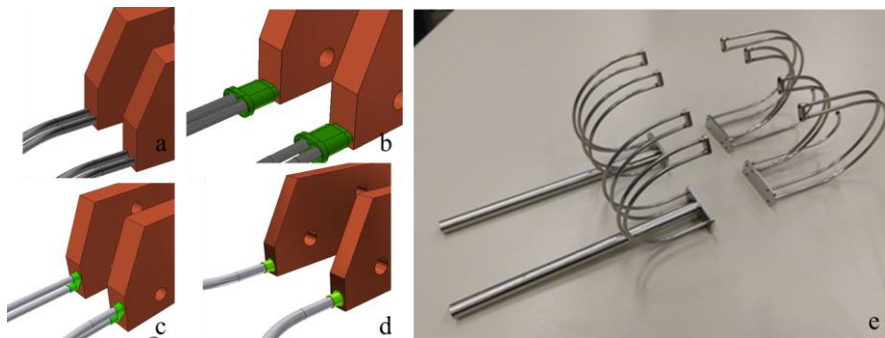


Figure 9. Left: four union options between pipes and cooling blocks – (a) brazed, (b) preliminary insert, (c) MANACA/EMA inserts, (d) QUATI/SAPUCAIA inserts. Right: (e) laser welded parts for MANACA/EMA circuit.

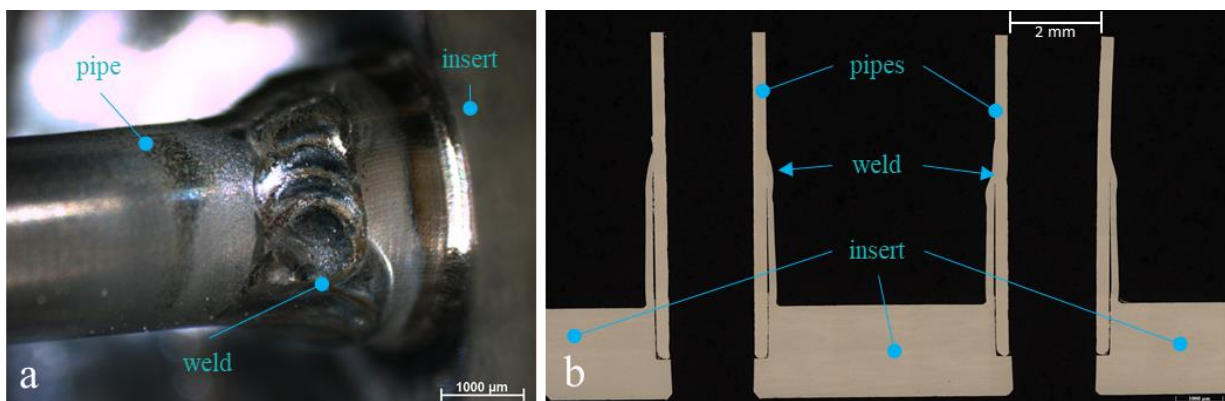


Figure 10 – Weld between pipes and insert for MANACÁ/EMA cooling systems.

#### 4.4. Final Brazing

After brazing the cooling blocks, machining the additive-manufactured manifold and laser welding the tubes, the final brazing of the full cryogenic cooling system was conducted. The brazed copper cooling blocks were cleaned and etched in an equivalent way to the first brazing step (see Section 4.2). Next, the stainless-steel inserts and the manifold were nickel (Ni) electroplated in a two-step procedure. In the first step, called Ni-Strike, the stainless-steel parts were etched at the same time that Ni deposition occurred. At this point, the Ni layer was only a few nanometres thick, but it helped improving the adhesion of the overall deposited layer. In the second step, called Ni-Watt, Ni was electroplated to the final thickness of 5  $\mu\text{m}$ .

To ensure the correct assembly to the final brazing, a set of alignment and clamping devices were designed and manufactured, and spring washers were used to allow the thermal expansion of the assembly without inducing plastic deformations. Special caution was taken about parts that were in contact but should not be brazed together. To avoid any issues, a thin layer of aluminium oxide suspension was laid down on these interface areas.

The vacuum brazing was performed using 0.1-mm-thick sheets of Cu-Ag brazing alloy (BAg-8), which has a melting temperature of 780°C. This brazing alloy was chosen due to its excellent copper and stainless-steel wettability, vacuum compatibility, and a melting temperature lower than that of the alloy used in the first brazing step (see Section 4.2). This final brazing was conducted in the same furnace and with the same parameters described for the cooling blocks. Again, a final leak test was performed to the final approval of the cooling system.

#### 4.5. Leak tests

All leak tests were performed in a leak detector equipment, model Agilent G8600-60002, calibrated to identify helium gas. Several devices were designed and manufactured to guarantee the reliability of the tests. The overall design guideline of these devices was to build a standard KF25 or KF40 reducer union to a suitable interface to the parts to be tested, in a compact and ease to manufacture way, as shown in Figure 11.

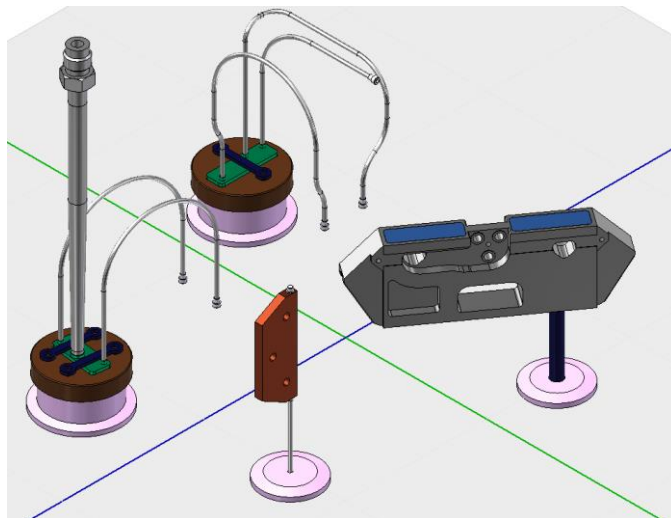


Figure 11 – Drawings of leak testing devices used in the the production of the cooling circuits for the HD-DCMs.

## 5 CONCLUSION

The proposed design of liquid nitrogen cooling circuits for the HD-DCM monochromators resulted from the stringent requirements in the thermal management and the dynamic positioning performance of their silicon optical elements. Indeed, sufficiently good heat extraction capacity and dynamics is obtained with an innovative architecture, based on: 1) a mechanically-decoupled solution between the main manifold and the crystal cooling blocks via thin distribution tubes; 2) a continuous and smooth flow path, with minimum interfaces, and sinusoidal and arterial-shaped circuits developed with CFD simulations; and 3) combined engineering and manufacturing processes.

The design aspects were presented and analyzed by computational simulations and a successful manufacturing process was fully developed. The two-step brazing process and the laser welding achieved the vacuum tightness and dimensional specifications. The additive manufacturing process proved to be essential to improve the machine performance, and an effective way to build pieces with complex internal channels, with vacuum and cryogenic compatibility. Two units are currently in operation and third and fourth units are being manufactured with small modifications due to the different geometric requirements of the new beamlines.

In this sense, the additive manufacturing can be further explored even in UHV application in future work and different projects. Regarding the HD-DCMs, options may include the introduction of internal voids in the main manifold, to relieve mass and improve dynamics even further, and printing also the copper parts, aiming at minimizing the number of steps and to optimizing curvatures in the internal paths.

## 6 Acknowledgements

The authors would like to gratefully acknowledge the funding by the Brazilian Ministry of Science, Technology and Innovation and the contributions of the LNLS team and the partner companies.

## 7 References

- Auricchio, M. M. B. Mei, P. R. Bagnato, O. 2019. "Soldering of silicon to Invar for double-crystal monochromators." *Journal of Synchrotron Radiation* 26 (5), doi:10.1107/S1600577519008191
- Bagnato, O. R. Francisco, F. R. Rosales, M. J. C., Manoel, F. E. 2011 "Development and Interfacial Analysis of Diffusion Bonding Between Copper and Stainless Steel for Applications in Ultra-High Vacuum". In *Proceedings of 21st Brazilian Congress of Mechanical Engineering – COBEM 2011*. Natal, Brazil.
- Caliari, R. "Studies on Flow-induced Vibrations for the New High-Dynamics DCM for Sirius." In *Proceedings of Mechanical Engineering Design of Synchrotron Radiation Equipment and Instrumentation – MEDSI 2016*, Barcelona, Spain.
- Chelton, D. B. "Cryogenic Data Book". Lawrence Berkeley National Laboratory. 2010.
- Incropera, F. E. A. et al. « Fundamentals of Heat and Mass Transfer". 7. ed. Jefferson: John Wiley & Sons, 2012.
- Lena, F. R. et al, 2021. "Copper Braid Heat Conductors for Sirius Cryogenic X-Ray Optics." Submitted to *Mechanical Engineering Design of Synchrotron Radiation Equipment and Instrumentation – MEDSI 2021*. Chicago, USA.
- Geraldes, R. R. et al, 2018. "The Status of The New High-Dynamic DCM for Sirius." In *Proceedings of Mechanical Engineering Design of Synchrotron Radiation Equipment and Instrumentation – MEDSI 2018*, Paris, France, pp. 147-152.
- Moreno, C. G. 2010. "Turbulence, Vibrations, Noise and Fluid Instabilities. Practical Approach". In book: *Computational Fluid Dynamics*. Edition: 1. Chapter: 5. Intech.
- Westfahl Jr. H. et al, 2018. "X-Ray Microscopy at Sirius, the New Brazilian Synchrotron Light Source." *Microscopy and Microanalysis*, 24(S2), 172-175. doi:10.1017/S1431927618013235.
- Wetering, N. v. d., 2019. "Flow-Induced Vibrations in the HD-DCM". Internal Report. CNPEM.
- Zluhan, B. Neustädter Jr., W. 2019. "Manufatura aditiva Metálica – Fusão Seletiva a Laser". Infocus Laser Systems.

## 8 Responsibility notice

The authors are the only responsible for the printed material included in this paper.